Supporting Information

Ultrathin Defect-Rich Co_3O_4 Nanosheets Cathode for High-Energy and Durable Aqueous Zinc Ion Battery

Yongzhuang Lu,[a] Jing Wang,[b] Siqi Zeng,[a] Lijun Zhou,[a] Wei Xu,[a] Dezhou Zheng,[a*] Jie Liu,[c] Yinxiang Zeng, [b*] and Xihong Lu[a,b*]

[a.] *School of Applied Physics and Materials, Wuyi University, Jiangmen, Guangdong 529020, P. R. China. E-mail: 523906991@qq.com (D. Zheng);*

[b.] *MOE MOE of the Key Laboratory of Bioinorganic and Synthetic Chemistry, The Key Lab of Low-carbon Chem & Energy Conservation of Guangdong Province, School of Chemistry, Sun Yat-Sen University, Guangzhou 510275, P. R. China. E-mail: zengyinx@mail2.sysu.edu.cn (Y. Zeng); luxh6@mail.sysu.edu.cn (X. Lu)*

[c.] *College of Chemistry and Chemical Engineering, Yantai University, Yantai 264005, P. R. China*

Experimental Section:

Preparation of Co_3O_4 and R-Co_3O_4 nanosheets: The synthesis of pristine Co_3O_4 included the hydrothermal process and a subsequent calcination. Firstly, a piece of carbon cloth (3×2 cm^2) was immerged in ethanol and sonicated for 15 min. 0.14 mol/L $Co(NO_3)_2 \cdot 6H_2O$, 0.28 mol/L NH_4F, and 0.71 mol/L urea were dissolved in distilled water to form a homogeneous solution. The solution was then transferred into a Teflon-lined autoclave and a piece of carbon cloth was then immersed into the solution. The autoclave was maintained at 120 °C for 6 h, and then naturally cool down at room temperature. The as-prepared sample was annealed in air at 350 °C for 2 h to obtain Co_3O_4. Further, the R-Co_3O_4 nanosheets were obtained by a solvothermal reduction method in ethylene glycol at 180 °C for 24 h. The mass loadings of pristine Co_3O_4 and R-Co_3O_4 nanosheets samples were 4.21 mg cm^{-2} and 3.86 mg cm^{-2} respectively, which were obtained by electronic scales (BT25S, 0.01 mg).

Material Characterization: The morphologies and compositions of the electrode materials were characterized using field-emission SEM (FESEM, JSM-6330F), transmission electron microscopy (TEM, FEI Tecnai G2 F30), Raman spectroscopy (Renishaw inVia), XPS (XPS, Nexsa, Thermo FS), AFM (SPM-9500J3) and XRD (Rigaku D-MAX 2200). The Co L-edge XANES spectra were collected at the photoemission end-station at beamline BL10B in the National Synchrotron Radiation Laboratory (NSRL) in Hefei, China. The surface area of the samples was calculated from nitrogen adsorption/desorption isotherms at 77 K that were obtained using a Brunauer–Emmett–Teller test (JW-BK100A).

Electrochemical Measurement: CV, charge-discharge measurements, and electrochemical impedance spectroscopy were conducted using an electrochemical workstation (PARSTAT MC). The electrochemical studies of individual electrodes were applied in a three-electrode cell, with a carbon rod counter electrode and a Hg/HgO reference electrode, in 6 M KOH saturated with $Zn(Ac)_2$ (~ 0.5 M $Zn(Ac)_2$) aqueous solution. The Zn//Co batteries with Co_3O_4 and R-Co_3O_4 cathodes were assembled using zinc plate anode with 6 M KOH saturated with $Zn(Ac)_2$ as electrolyte.

Calculations:

The areal capacity (C_a) and specific capacity (C_s) were calculated from the galvanostatic curve using the following equations:

$$C_a = \frac{\int_0^{\Delta t} I dt}{S} \quad (1)$$

$$C_s = \frac{\int_0^{\Delta t} I dt}{m} \quad (2)$$

Where C_a is the areal capacity (mAh cm^{-2}), C_s is the specific capacity (mAh g^{-1}), I (mA) is the applied discharging current, Δt (h) is the discharging time, S (cm^2) is the area of the cathode and m (g) is the mass loading of the cathode.

Specific energy density E and specific power density P of the cell were obtained from the following equations:

$$E = \int_{V_1}^{V_1} C_s dV \quad (3)$$

$$P = \frac{E}{1000 \times \Delta t} \quad (4)$$

Where E (Wh kg^{-1}) is the energy density, P is the power density (kW kg^{-1}), V (V) is the working potential, C_s is the specific capacity (mAh g^{-1}), and Δt (h) is the discharging time.

Alternatively, Volumetric energy density and power density of the device were obtained from the following equations:

$$E = \int_{V_1}^{V_1} \frac{C_a}{d} dV \quad (5)$$

$$P = \frac{E}{1000 \times \Delta t} \quad (6)$$

where E (Wh cm^{-3}) is the energy density, P (W cm^{-3}) is the power density, C_a is the areal capacitance (mAh cm^{-2}) obtained from Equation (1), V (V) is the working potential, d (cm) is the thickness of the device (cm), and Δt (h) is the discharging time.

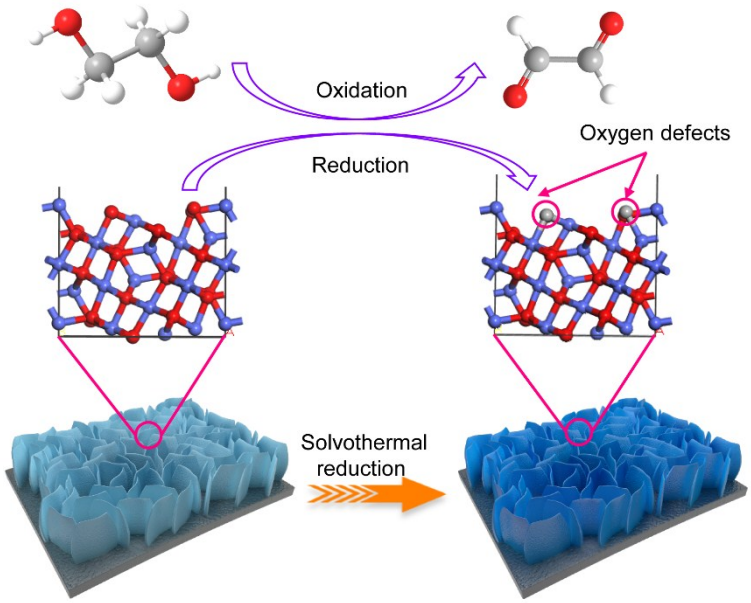

Fig. S1. The schematic illustration of creating oxygen vacancy defects on the surface of ultrathin Co_3O_4 nanosheets.

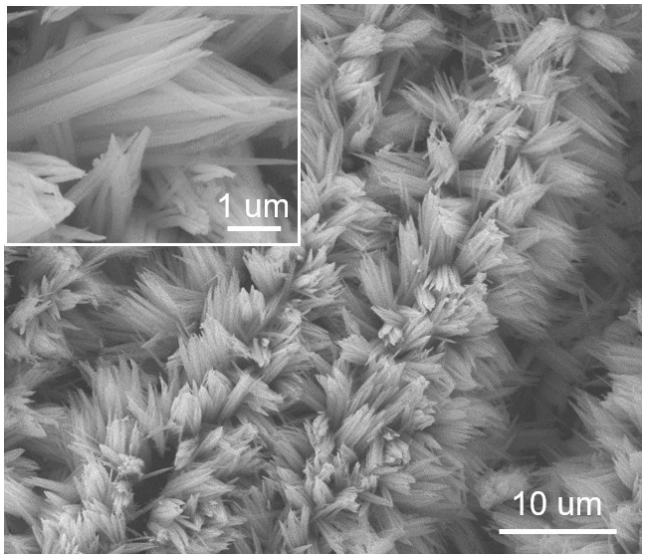

Fig. S2. SEM images of the pristine Co_3O_4 nanowire sample.

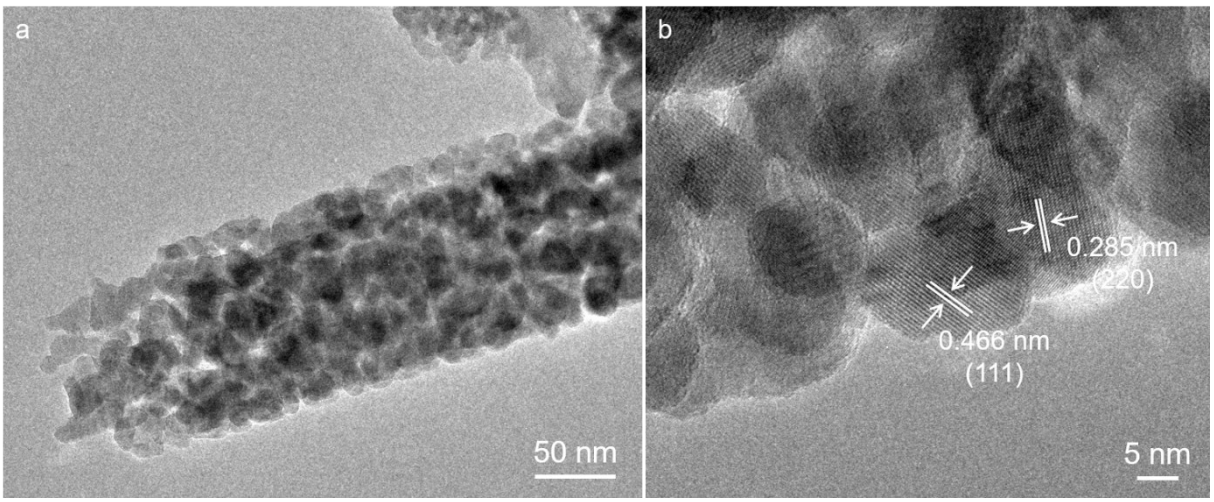

Fig. S3. (a) TEM image and (b) HRTEM image of the pristine Co_3O_4 nanowire sample.

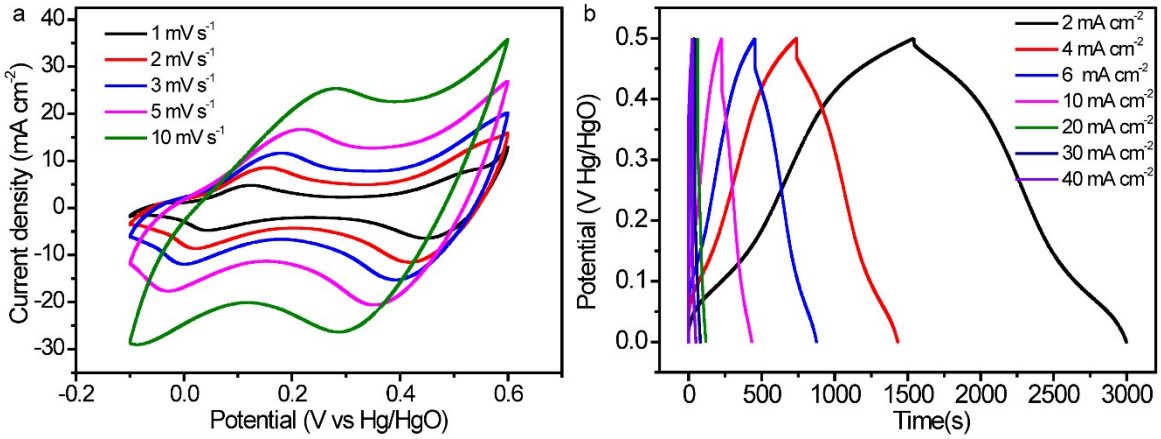

Fig. S4. (a) CV curves at various scan rates; (b) charge-discharge profiles at different current densities for the R-Co_3O_4 nanowire electrode.

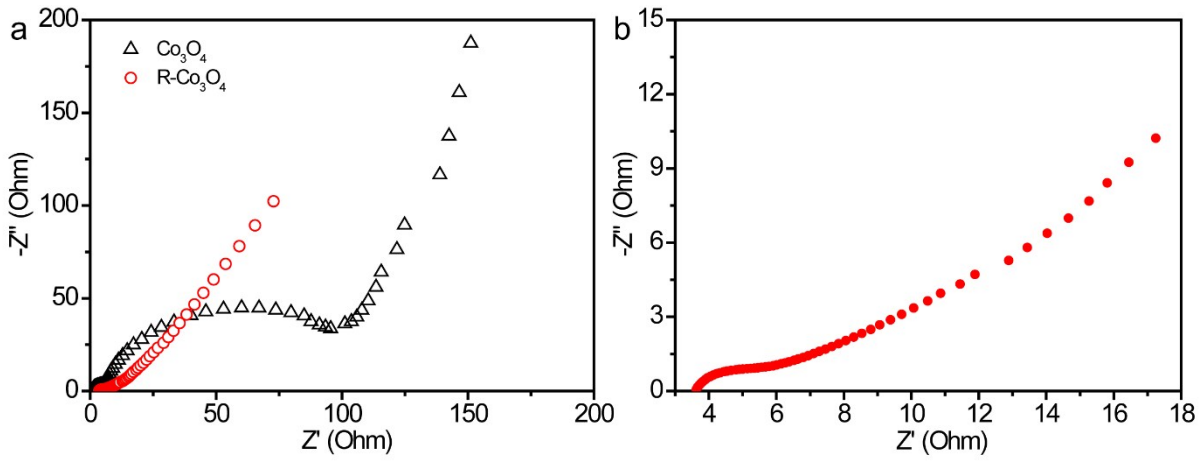

Fig. S5. (a) Nyquist plots of the pristine Co_3O_4 and R-Co_3O_4 electrodes. (b) Enlarged Nyquist plot of the R-Co_3O_4 electrode.

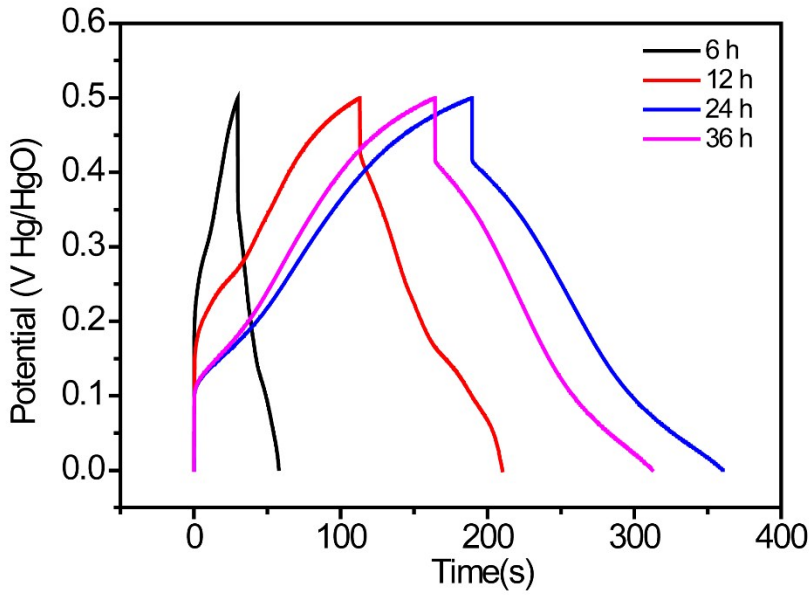

Fig. S6. Charge-discharge profiles for the R-Co_3O_4 nanowire electrodes reduced with different times at 10 mA cm^{-2}.

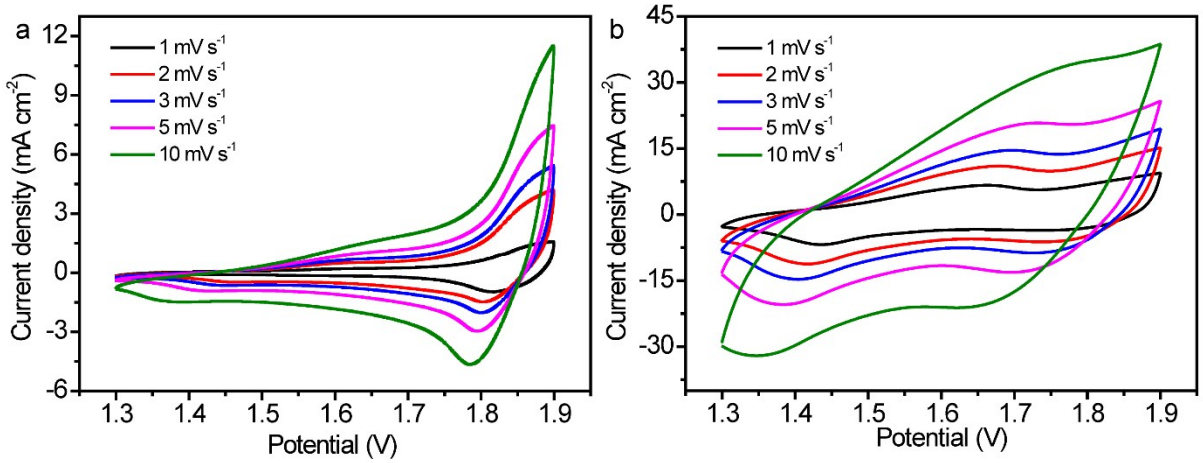

Fig. S7. CV curves of the Zn//Co batteries with (a) pristine Co_3O_4 and (b) R-Co_3O_4 cathodes at various scan rates.

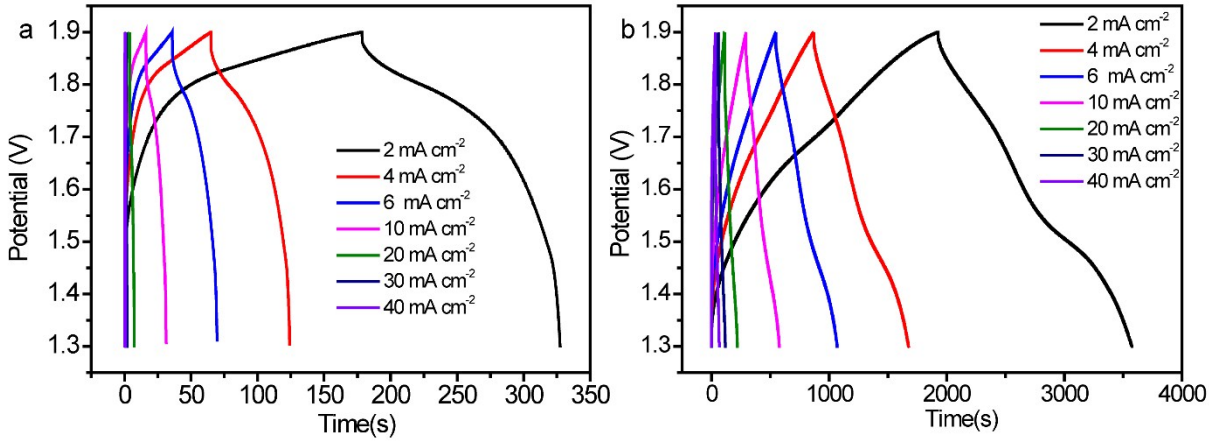

Fig. S8. Charge-discharge profiles of the Zn//Co batteries with (a) pristine Co_3O_4 and (b) R-Co_3O_4 cathodes at various current densities.

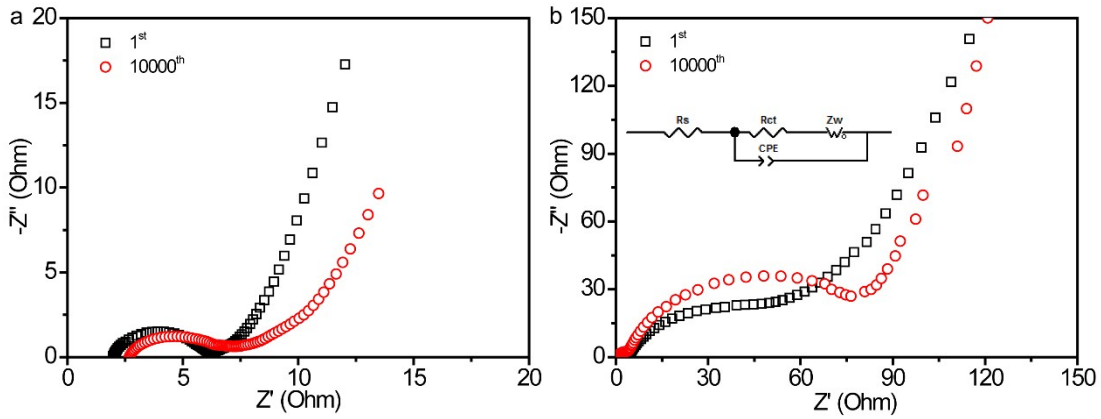

Fig. S9. Nyquist plots of the Zn//Co batteries with (a) R-Co_3O_4 and (b) pristine Co_3O_4 cathodes; and the corresponding equivalent circuit diagram of the Zn//Co batteries is inset in the Fig. S9b.

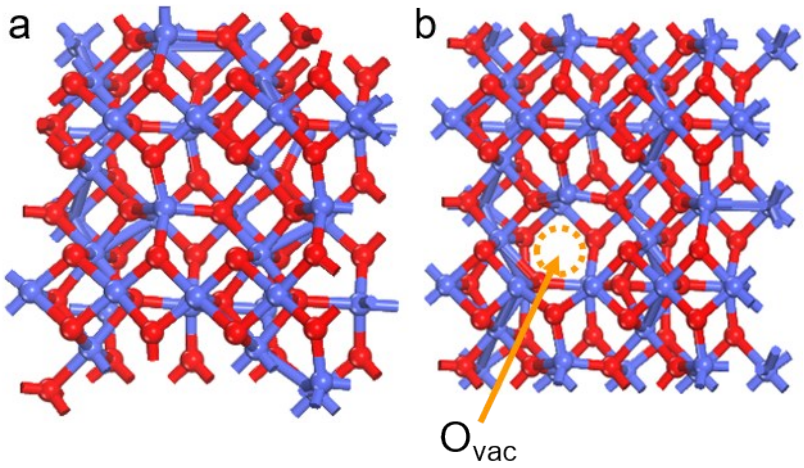

Fig. S10. Constructed models of Co_3O_4 (311) surfaces with (a) perfect surface (presenting Co_3O_4) and (b) a surface with an oxygen vacancy (presenting R-Co_3O_4).

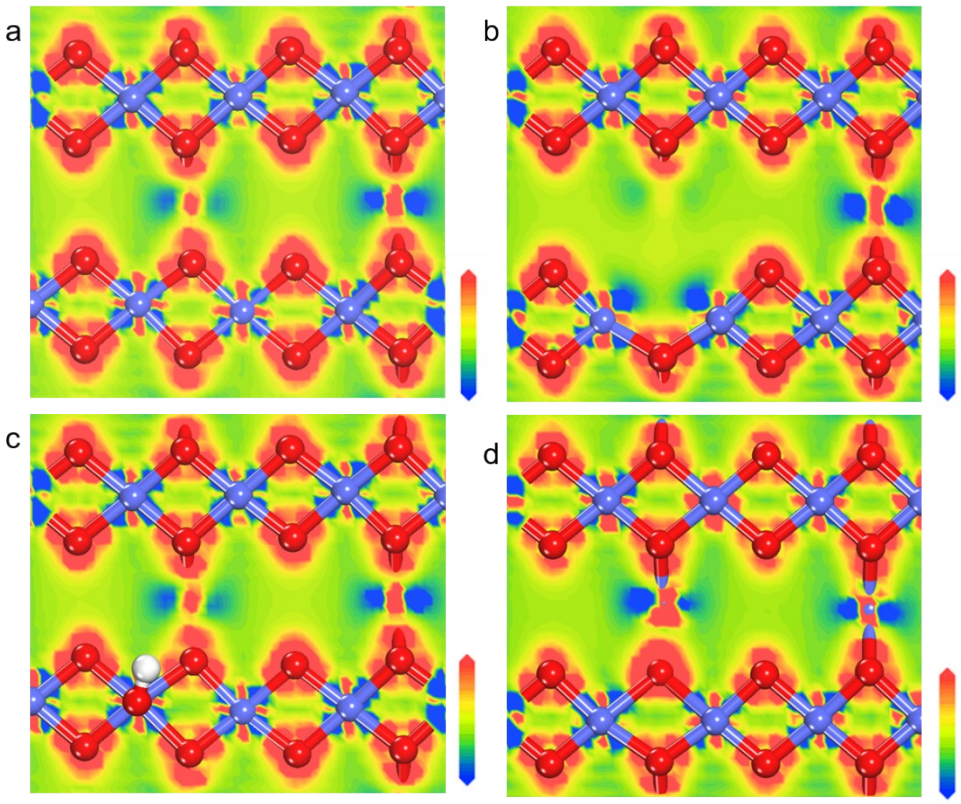

Fig. S11. The top-view electron density difference of (a) pristine Co_3O_4, (b) R-Co_3O_4 with one oxygen vacancy, (c) pristine Co_3O_4 after adsorption of OH^-, and (d) R-Co_3O_4 with one oxygen vacancy after adsorption of OH^-.

Table S1. Comparison of our Zn//R-Co_3O_4 battery with some recently reported Zn-based batteries.

Battery	Electrolyte	Capacity (mAh g^{-1})
Zn//R-Co_3O_4	6 M KOH saturated with $Zn(Ac)_2$	240.8 (0.53 A g^{-1}); 159.8 (5.3 A g^{-1}); 96.3 (10.5 A g^{-1})
Zn//Co_3O_4	6 M KOH saturated with $Zn(Ac)_2$	19.7 (0.48 A g^{-1}); 4.72 (4.8 A g^{-1})
Ni_3S_2//Zn[1]	1 M KOH + 0.02 M $Zn(Ac)_2$	148 (0.2 A g^{-1}); 68 (5 A g^{-1})
Zn@CF//Co_3O_4[2]	1 M KOH + 0.001 M $Zn(Ac)_2$	168 (1 A g^{-1}); 78 (10 A g^{-1})
Zn//Co(III) rich-Co_3O_4[3]	2 M $ZnSO_4$ + 0.2 M $CoSO_4$	200 (0.5 A g^{-1}); 91 (5 A g^{-1})
CC-CF@NiO//CC-CF@ZnO[4]	2 M KOH saturated with ZnO	203 (0.96 A g^{-1}); 78 (10 A g^{-1})
Zn//CuHCF[5]	0.02 M $ZnSO_4$	54 (0.06 A g^{-1}); 43.7 (0.6 A g^{-1})
Zn//ZnHCF[6]	3 M $ZnSO_4$	66.5 (0.06 A g^{-1}); 29.3 (1.2 A g^{-1})
Zn//$Na_3V_2(PO_4)_2F_3$[7]	2 M $Zn(CF_3SO_3)_2$	60 (0.2 A g^{-1}); 33 (3 A g^{-1})
Zn//$Na_3V_2(PO_4)_3$[8]	0.5 M $Zn(CH_3COO)_2$	97 (0.05 A g^{-1}); 58 (1 A g^{-1})
Zn//VS_2[9]	1 M $ZnSO_4$	159.1 (0.1 A g^{-1}); 115.5 (2 A g^{-1})
Zn//$Na_{0.33}V_2O_5$[10]	3 M $Zn(CF_3SO_3)_2$	173.4 (0.5 A g^{-1}); 96.4 (2 A g^{-1})
Zn//a-MnO_2/CNT battery[11]	0.3 M $ZnSO_4$ + 0.015 M $MnSO_4$	145 (0.1 A g^{-1}); 97 (0.25 A g^{-1})
Zn//$ZnMn_2O_4$[12]	2 M $Zn(CF_3SO_3)_2$	~ 150 (0.05 A g^{-1}); 72 (2 A g^{-1})
Zn//Mn_3O_4[13]	2 M $ZnSO_4$ + 0.1 M $MnSO_4$	185 (0.3 A g^{-1}); 125 (0.5 A g^{-1})
Zn//MnO_2@CNT[14]	2 M $Zn(CF_3SO_3)_2$-PVA	188 (0.1 A g^{-1}); 45 (2 A g^{-1})
Zn//MnO_2[15]	2 M $ZnSO_4$ + 0.2 M $MnSO_4$	~235 (0.754 A g^{-1}); 43 (1.885 A g^{-1})

Reference:

1. P. Hu, T. Wang, J. Zhao, C. Zhang, J. Ma, H. Du, X. Wang and G. Cui, *ACS Appl. Mater. Interfaces*, 2015, **7**, 26396-26399.
2. X. Wang, F. Wang, L. Wang, M. Li, Y. Wang, B. Chen, Y. Zhu, L. Fu, L. Zha, L. Zhang, Y. Wu and W. Huang, *Adv. Mater.*, 2016, **28**, 4904-4911.
3. L. Ma, S. Chen, H. Li, Z. Ruan, Z. Tang, Z. Liu, Z. Wang, Y. Huang, Z. Pei and J. A. Zapien, *Energy Environ. Sci.*, 2018, **11**, 2521-2530.
4. J. Liu, C. Guan, C. Zhou, Z. Fan, Q. Ke, G. Zhang, C. Liu and J. Wang, *Adv. Mater.*, 2016, **28**, 8732-8739.
5. R. Trocoli and F. La Mantia, *ChemSusChem*, 2015, **8**, 481-485.
6. L. Zhang, L. Chen, X. Zhou and Z. Liu, *Sci. Rep.*, 2015, **5**, 18263.
7. W. Li, K. Wang, S. Cheng and K. Jiang, *Energy Storage Mater.*, 2018, **15**, 14-21.
8. G. Li, Z. Yang, Y. Jiang, C. Jin, W. Huang, X. Ding and Y. Huang, *Nano Energy*, 2016, **25**, 211-217.
9. P. He, M. Yan, G. Zhang, R. Sun, L. Chen, Q. An and L. Mai, *Adv. Energy Mater.*, 2017, **7**, 1601920.
10. P. He, G. Zhang, X. Liao, M. Yan, X. Xu, Q. An, J. Liu and L. Mai, *Adv. Energy Mater.*, 2018, **8**, 1702463.
11. F. Mo, H. Li, Z. Pei, G. Liang, L. Ma, Q. Yang, D. Wang, Y. Huang and C. Zhi, *Science Bulletin*, 2018, **63**, 1077-1086.
12. N. Zhang, F. Cheng, Y. Liu, Q. Zhao, K. Lei, C. Chen, X. Liu and J. Chen, *J. Am. Chem. Soc.*, 2016, **138**, 12894-12901.
13. C. Zhu, G. Fang, J. Zhou, J. Guo, Z. Wang, C. Wang, J. Li, Y. Tang and S. Liang, *J. Mater. Chem. A*, 2018, **6**, 9677-9683.
14. K. Wang, X. Zhang, J. Han, X. Zhang, X. Sun, C. Li, W. Liu, Q. Li and Y. Ma, *ACS Appl. Mater. Interfaces*, 2018, **10**, 24573-24582.
15. W. Sun, F. Wang, S. Hou, C. Yang, X. Fan, Z. Ma, T. Gao, F. Han, R. Hu, M. Zhu and C. Wang, *J. Am. Chem. Soc.*, 2017, **139**, 9775-9778.